

Optical Anisotropy and Conformational Analysis of Styrene-Methyl Methacrylate Block Copolymers in Dilute Solutions

E. Saiz

Departamento de Química Física, Universidad de Alcalá de Henares, 28871 Madrid, Spain

G. Floudas[†] and G. Fytas^{*}

Research Center of Crete, P.O. Box 1527, 71110 Heraklion, Crete, Greece

Received February 22, 1991; Revised Manuscript Received June 12, 1991

ABSTRACT: The effective optical anisotropy $\langle \gamma^2 \rangle$ of polystyrene-poly(methyl methacrylate) (PS-PMMA) diblock and PMMA-PS-PMMA triblock copolymers in dioxane solutions has been obtained from the depolarized Rayleigh spectra (DRS) using a planar Fabry-Perot interferometer. The DRS technique selectively samples the PS block: the PMMA block is nearly invisible. The PS chain in the diblock and triblock copolymers suffers a substantial conformational change when dissolved in dioxane as indicated respectively by the low (22 Å⁶) and high (61 Å⁶) optical anisotropy compared to the homopolymer chain (38 Å⁶). The conformational analysis of PS block based on the isomeric state theory constitutes a confirmation of the experimental $\langle \gamma^2 \rangle/x$ obtained from DRS and the overall hydrodynamic radius R_H obtained by photon correlation spectroscopy. The differences in $\langle \gamma^2 \rangle/x$ exhibited by the PS chain and the overall dimensions in the diblock and triblock solutions in dioxane are due to conformational changes mainly in the racemic units that change from a strong preference for the compact gg conformation in the case of PS-PMMA to a predilection for the most extended and anisotropic tt conformation in the PMMA-PS-PMMA copolymer.

Introduction

Recently, we have employed depolarized Rayleigh spectroscopy to measure the optical anisotropy of flexible polymers¹⁻³ and rigid oligomers⁴ in solution. The knowledge of the intrinsic molecular anisotropy γ^2 of the rigid nematogens⁴ or the average optical anisotropy per repeating unit $\langle \gamma^2 \rangle/x$ (x being the degree of the polymerization of the polymers¹⁻³) was highly useful for determination of conformational parameters of the studied materials. Optical anisotropy is usually treated as a constitutive property, and as such it can be a sensitive index of chain conformation and microstructure. For poly(phenylmethylsiloxane),² it was recently shown that $\langle \gamma^2 \rangle/x$ can vary with chain tacticity, in agreement with rotational isomeric state (RIS) calculations.^{5,6}

Chain conformation is generally an important issue in polymer science. Copolymers, consisting of incompatible blocks, can show interesting configurations in solution depending mainly on the heterosegmental interactions and solvent quality with regard to each block component.⁷ Even if intermolecular association (micelles), typical of a selective solvent, is prevented, the single copolymer chain can be approximated by different models.^{8,9} The conformation of an A-B diblock copolymer is usually characterized in terms of the radius of gyration of the A and/or B block and the overall dimension of the copolymer. On the basis of these measurements, for the diblock polystyrene (PS)-poly(methyl methacrylate) (PMMA) in toluene, a common solvent for both parent homopolymers, the PS block has similar conformation to its homopolymer state.^{8,9} Alternatively, the compact size of the PMMA block, as measured by neutron scattering, suggests a near- θ configuration for PMMA.⁹ For more than two blocks, like a triblock PMMA-PS-PMMA (BAB) copolymer¹⁰ also in toluene, the central A is more extended than

the equivalent A homopolymer. The overall dimension of the triblock copolymer, obtained from intrinsic viscosity measurements, is also larger than its diblock counterpart.

In an effort to elucidate chain conformation in solution, using Fabry-Perot interferometry we have measured for the first time to our knowledge the intrinsic optical anisotropy $\langle \gamma^2 \rangle/x$ of the diblock PS-PMMA and triblock PMMA-PS-PMMA copolymer in dilute dioxane solution.¹¹ This solvent, common to both homopolymers, was chosen for its low (relative to toluene) depolarized Rayleigh intensity.⁴ For these copolymers, PMMA block is almost invisible owing to the large difference in the anisotropic scattering intensity for PMMA and PS. Thus, the depolarized Rayleigh scattering technique selectively samples the PS block. The overall dimension of the copolymer was estimated by measuring the hydrodynamic radius R_H at infinite dilution using photon correlation spectroscopy. We complement the experimental results with a conformational analysis of the PS subchain for a quantitative characterization of its structural changes as perturbed by the side PMMA blocks in a given solvent.

Experimental Section

The molecular characteristics of the sample used in the present study are given in Table I. The effective mean-square optical anisotropy $\langle \gamma^2 \rangle/x$ per monomer unit can be computed from

$$\langle \gamma^2 \rangle/x = 15(\lambda_0/2\pi)^4 f(n)^{-1} (R_{VH}/\rho) \quad (1)$$

where λ_0 is the wavelength of light in vacuo, ρ is the number density of the anisotropic monomer units, and $f(n) = ((n^2 + 2)/3)^2$ is the second-power spherical Lorentz local field correction.¹² The absolute depolarized Rayleigh ratio R_{VH} is computed from the depolarized intensity I_{VH} attributed to the solute molecules with volume fraction ϕ ; i.e., $I_{VH} = I_{\text{solu}} - (1 - \phi)I_{\text{solu}}$. The intensities of the solution (I_{solu}) and the inert solvent (I_{solu}) were obtained from numerical integration of their experimental low-frequency depolarized Rayleigh spectra $I_{VH}(\omega)$. The latter were taken at a scattering angle of 90° by using a plane Fabry-Perot interferometer with a free spectral range of 40 cm⁻¹, as described elsewhere.⁴ The generally high-frequency component of the collision-induced scattering¹² appears in the nonzero background.

^{*} To whom correspondence should be addressed.

[†] Present address: Department of Chemical Engineering, Imperial College, London SW7 2BY, England.

Table I
Molecular Characteristics, Depolarized Rayleigh Intensities, and Optical Anisotropies of Block Copolymers in Solution at 25 °C

sample	M_w	f_{PS}	$(R_{VH}/\rho)/10^{-27} \text{ cm}^2$	$(\langle \gamma^2 \rangle/x)/\text{\AA}^6$
PS in CCl_4	3×10^5		1.3 ± 0.1	38 ± 2
PS-PMMA in CCl_4	8.3×10^4	0.68	1.35 ± 0.05	39 ± 1
PS-PMMA in dioxane	8.3×10^4	0.68	0.7 ± 0.1	22 ± 2
PMMA-PS-PMMA in dioxane	1.04×10^5	0.59	2.0 ± 0.1	61 ± 2

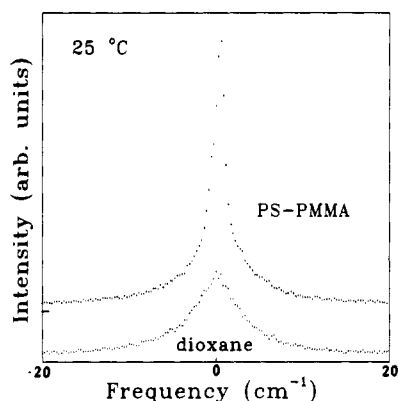


Figure 1. Depolarized Rayleigh spectra of PS-PMMA in dioxane and neat dioxane at 25 °C.

Two experimental spectra of the solvent dioxane and of the diblock PS-PMMA dioxane solution at 25 °C are shown in Figure 1. Depolarized Rayleigh measurements were carried out in the low-polymer concentration region ($\sim 1\%$) to minimize intermolecular orientation correlations as indicated by the insensitivity of R_{VH}/ρ to variations of the solute concentration.

Dynamic Light Scattering Results

Optical Anisotropy. We measured first the $\langle \gamma^2 \rangle/x$ for atactic PS ($M_w = 3 \times 10^5$) in CCl_4 to verify the RIS result.⁶ We obtained $\langle \gamma^2 \rangle/x = 38 \pm 2 \text{ \AA}^6$, in good agreement with the theoretical value. As opposed to the atactic PS chain with $R_{VH}/\rho = 1.3 \times 10^{-27} \text{ cm}^2$, the anisotropic scattering of bulk PMMA ($R_{VH}/\rho = 0.04 \times 10^{-27} \text{ cm}^2$)¹³ is very weak, and hence the PMMA block in a PMMA-PS block copolymer is nearly invisible. Thus for the PS-PMMA diblock copolymer in CCl_4 , a selective solvent for the PS subchain, we expect a $\langle \gamma^2 \rangle/x$ value similar to that of the homopolymer PS in CCl_4 . The depolarized Rayleigh ratio $R_{VH}/(\rho f_{PS})$ of the diblock chain with weight fraction f_{PS} ($=0.68$) was found to be very close to the R_{VH}/ρ for PS homopolymer. The diblock copolymer in CCl_4 is organized in micelles (as inferred from polarized light scattering measurements), with the PMMA block forming the interior core. The PS subchain, which exudes out forming the shell, has a conformation similar to that of the homopolymer PS; the microstructure of PS, examined by high-resolution NMR, is the same in both homopolymer and block copolymer. We therefore feel justified in assuming that the depolarized light scattering from PS-PMMA copolymers is predominantly due to the PS block and the $\langle \gamma^2 \rangle/x$ is an index of the conformations of this block.

In dioxane, which is a common solvent for both blocks, the two copolymers form molecularly dispersed solutions, verified also by polarized light scattering measurements. However, as we see below, dioxane is a better solvent for PMMA than for PS. The results of the present depolarized Rayleigh study are summarized in Table I. As already mentioned, in the computation of $\langle \gamma^2 \rangle/x$ we have used the weight fraction f of PS in the block copolymers and neglected the anisotropic contribution of PMMA.

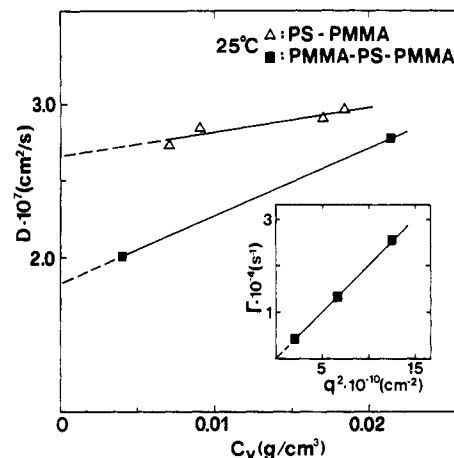


Figure 2. Translational diffusion coefficient for diblock PS-PMMA and triblock PMMA-PS-PMMA copolymer versus polymer concentration in dioxane at 25 °C. The diffusional character of the relaxation rate $\Gamma (=Dq^2)$ for a 0.004 g/cm³ triblock/dioxane solution is shown in the insertion.

For the diblock/dioxane dilute solution, this low value clearly supports the conjecture that the PS subchain is rather compact with preference for *gg* conformations.¹⁴ Conversely, the high $\langle \gamma^2 \rangle/x$ of the center PS block in the triblock/dioxane solution is in accord with the larger hydrodynamic volume and larger radius of gyration of PS in PMMA-PS-PMMA/toluene solution¹⁰ as compared respectively with an equivalent diblock and homopolymer PS. In the subsequent section, the conformational analysis of PS block constitutes a confirmation of the experimental $\langle \gamma^2 \rangle/x$ values. In the next subsection, we complement the anisotropic scattering data with dynamic polarized light scattering measurements of the overall hydrodynamic radius of the copolymer chain in dioxane.

Overall Dimension. The translational diffusion coefficient D of the copolymer chain in dilute dioxane solutions was obtained from the intensity time correlation function $G(q,t)$ measured at different concentrations of three scattering angles (q is the scattering wave vector). The $G(q,t)$ was recorded by the log-lin Malvern correlator (K7027) over the time range 10^{-6} – 10^{-2} s. The net correlation function $(G(q,t)/A - 1)^{1/2}$, with A being the measured baseline, is represented by

$$(G(q,t)/A - 1)^{1/2} = b \exp(-Dq^2t) \quad (2)$$

where b is a fitting parameter.

Figure 2 shows the concentration dependence of D for the diblock and triblock copolymers where the insert in the same figure underlines the q^2 dependence of the relaxation rate $\Gamma = Dq^2$ (eq 2). The variation of D (obtained from the angular dependence of Γ) with solute concentration in dilute homopolymer solutions is usually described¹⁵ by the linear dependence

$$D = D_0(1 + k_D c) \quad (3)$$

where k_D is the concentration coefficient and D_0 is the translational diffusion of the chain at infinite dilution. The values of these fitting parameters are $D_0 = 2.66 \times 10^{-7} \text{ cm}^2/\text{s}$ and $k_D = 6 \text{ cm}^3/\text{g}$ for the diblock and $D_0 = 1.84 \times 10^{-7} \text{ cm}^2/\text{s}$ and $k_D = 23.5 \text{ cm}^3/\text{g}$ for the triblock solution. The equivalent hydrodynamic radius $R_H = k_B T / 6\pi\eta_0 D_0$, with η_0 being the viscosity of the solvent, amounts to 74 and 108 Å respectively for the diblock and triblock chain.

The triblock appears to be larger than the diblock chain, and this disparity cannot be accounted for by differences in their molecular weights (Table I). This finding supports

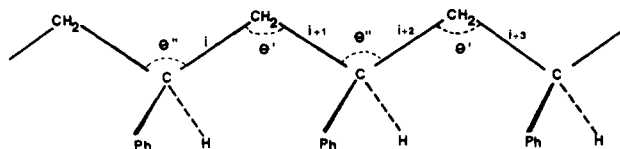


Figure 3. A segment of the PS chain shown in its planar all-trans conformation.

the intrinsic viscosity data¹⁰ on the same copolymers reported previously and the larger $\langle \gamma^2 \rangle / x$ of the PS block in the triblock copolymer, with both experiments being compatible with an extended-chain conformation. The k_D values are also along this line.

For homopolymer solutions, k_D incorporates both thermodynamic and kinetic effects:

$$k_D = 2A_2M - k_f + v \quad (4)$$

where k_f is the concentration factor for the friction coefficient, A_2 is the second virial coefficient, and v is the specific volume of the polymer. According to eq 4, k_D assumes positive values for relatively high molecular weights in good solvents ($A_2 > 0$). Although the interpretation is not that straightforward for copolymers, the same chemical nature of the present copolymers, however, still allows a connection between solvent quality and the sign of the k_D parameter. For triblock, the large positive k_D is consistent with the more extended-chain conformation as opposed to the diblock copolymer. We next attempt a quantitative conformational characterization of the PS subchain in the two copolymers.

Conformational Analysis

All the data required for the present work were taken from a previous analysis of PS reported by Flory and co-workers.^{6,16} Thus bond lengths of 1.53 Å with bond angles $\theta' = 114^\circ$ and $\theta'' = 112^\circ$ were used for the polymeric skeleton (see Figure 3). A two-state rotational model was used with the rotational isomers located at⁶ $(\langle \varphi_i \rangle, \langle \varphi_{i+1} \rangle) = (20, 20), (5, 110), (110, 5),$ and $(90, 90)$ respectively for conformations tt, tg, gt, and gg of the meso diad and $(\langle \varphi_i \rangle, \langle \varphi_{i+1} \rangle) = (10, 10), (20, 90), (90, 20),$ and $(105, 105)$ for the same conformations of a racemic unit. The statistical weight matrices are

$$U' = \begin{bmatrix} 1 & 1 \\ 1 & 0 \end{bmatrix} \quad (5a)$$

for the pair of bonds $\text{CH}_2\text{-C-CH}_2$, and

$$U_m'' = \begin{bmatrix} \omega'' & 1/\eta \\ 1/\eta & \omega/\eta^2 \end{bmatrix} \quad \text{and} \quad U_r'' = \begin{bmatrix} 1 & \omega'/\eta \\ \omega'/\eta & 1/\eta^2 \end{bmatrix} \quad (5b)$$

respectively for the meso and racemic configurations of the pair of bonds $\text{C-CH}_2\text{-C}$.

The statistical weights were computed as the product of a preexponential factor times a Boltzmann exponential of their respective conformational energy. Thus

$$\eta = 0.8 \exp(-E_\eta/RT) \quad \text{with } E_\eta \approx -0.4 \text{ kcal mol}^{-1} \quad (6a)$$

$$\omega = 1.3 \exp(-E_\omega/RT) \approx \omega' = 1.3 \exp(-E_{\omega'}/RT) \quad (6b)$$

with $E_\omega \approx E_{\omega'} \approx 2.0 \text{ kcal mol}^{-1}$

$$\omega'' = 1.8 \exp(-E_{\omega''}/RT) \quad \text{with } E_{\omega''} \approx 2.2 \text{ kcal mol}^{-1} \quad (6c)$$

Two contributions to the anisotropic part of the polarizability tensor of the polymer, α_i and α_{i+1} , are required for the two kinds of skeletal bonds contained in the repeat

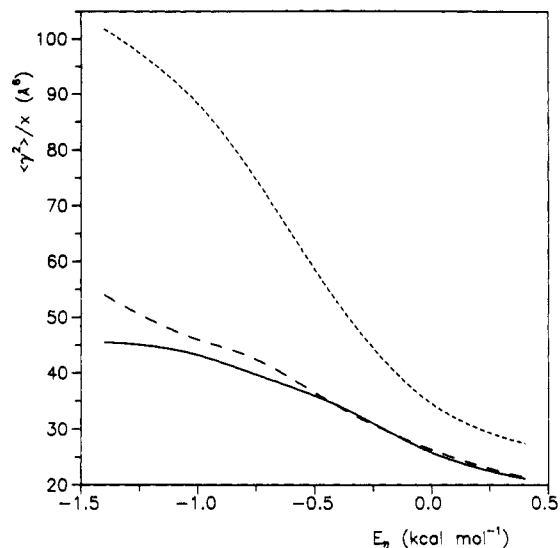


Figure 4. Mean-square optical anisotropy per repeat unit $\langle \gamma^2 \rangle / x$ as a function of the conformational energy E_η for $E_{\omega'} = 0$ (dotted line), 2.0 (dashed line), and 4.0 (solid line) kcal mol⁻¹. Computations were performed at 25 °C with $E_\omega = E_{\omega'} = 2.0$ kcal mol⁻¹. Results shown are averages over 20 independently generated Monte Carlo chains with $w_m = 0.5$; standard errors on the averages are ca. 1–2%.

unit of the chain, i.e., bonds C-CH_2 like i in Figure 3 and $\text{CH}_2\text{-C}$ like $i+1$ in the same figure. Taking into account that the chain of PS can be schematically obtained by addition of molecules of cumene, $\text{C}_6\text{H}_5\text{CH}(\text{CH}_3)_2$, with elimination of molecules of methane for which $\alpha_M = 0$, the tensor for one repeat unit of the polymer can be identified with that of the cumene molecule; this can be achieved by taking $\alpha_i = \alpha_{\text{cumene}}$ and $\alpha_{i+1} = 0$. Thus, according to the results of Suter and Flory⁶

$$\hat{\alpha}_i = \begin{bmatrix} -1.367 & -1.825 & 0.778 \\ -1.825 & 0.099 & -1.153 \\ 0.778 & -1.153 & 1.277 \end{bmatrix} \text{Å}^3$$

written in the coordinate system affixed to skeletal bond i .

The calculations were performed according to standard procedures of the matrix multiplication scheme.^{5,17} Thus, chains containing up to $x = 200$ repeat units (i.e., $n = 2x = 400$ skeletal bonds) were generated with a Bernoullian distribution of meso and racemic centers as to produce a predetermined fraction of meso diads w_m . All the results shown below for heterotactic chains (i.e., $0 < w_m < 1.0$) are averages over the values computed for 20 independently generated chains; typical standard errors of these averages are ca. 1–2%. Mean-square values of optical anisotropies $\langle \gamma^2 \rangle$ and end-to-end distance $\langle r^2 \rangle_0$ were computed and transformed into the ratios $\langle \gamma^2 \rangle / x$ and $C_n = \langle r^2 \rangle_0 / nl^2$ where l represents the length of the skeletal C-C bond. Both ratios increase with increasing x but reach asymptotic limits for $x = 50\text{--}100$. All the results reported below were computed at $x = 200$, for which the differences with the values extrapolated to $x \rightarrow \infty$ are negligible, mainly in the cases of heterotactic chains.

Some exploratory calculations were performed to check the sensitivity of the calculated magnitudes to the conformational energies. They proved that both $\langle \gamma^2 \rangle / x$ and C_n are sensitive to E_η and to $E_{\omega'}$ while the incidence of either E_ω or $E_{\omega''}$ is almost negligible. The variation of $\langle \gamma^2 \rangle / x$ and C_n of heterotactic chains having $w_m = 0.5$ with both E_η and $E_{\omega'}$ is shown respectively in Figures 4 and 5.

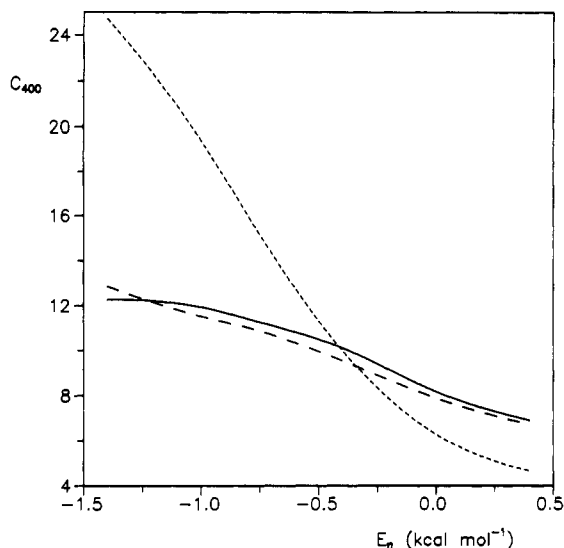


Figure 5. Characteristic ratios $\langle r^2 \rangle_0/nl^2$ for chains containing $n = 400$ skeletal bonds (i.e., $x = n/2 = 200$ repeat units) as a function of the conformational energy E_η . See legend for Figure 4.

It may seem surprising that there is a large difference between the values computed with $E_{\omega''} = 0$ and $E_{\omega''} + 2.0$ kcal mol $^{-1}$ as compared with the small variation produced by a further increase of $E_{\omega''}$ to 4.0 kcal mol $^{-1}$. Of course, the reason for this behavior is that ω'' decreases exponentially with increasing $E_{\omega''}$ and, once it reaches a value small enough as to be negligible compared with the other statistical weights, any further increase of the energy has no practical effect on the value of ω'' .

A comparison between Figures 4 and 5 indicates that the behavior of these two magnitudes is quite similar; they both increase with increasing values of the statistical weight η (i.e., with decreasing energy E_η). Thus, the polymeric chain expands from $C_n \approx 5-6$ at $E_\eta = 0.5$ to $C_n \approx 13-25$ (depending on the value of $E_{\omega''}$) at $E_\eta = -1.5$ kcal mol $^{-1}$, and at the same time it becomes more anisotropic, changing from $\langle \gamma^2 \rangle/x \approx 20-30$ to 50–100 Å 3 for the same variation of E_η .

The experimental values $\langle \gamma^2 \rangle/x \approx 39$ Å 3 measured for PS chains and for the PS-PMMA diblock copolymer in CCl $_4$ solutions at 25 °C are in good agreement with previous determinations 6 carried out in the same conditions of solvent and temperature although with different experimental equipment. As Suter and Flory 6 showed, these values can be reproduced with the set of energies $E_\eta = -0.4$ and $E_{\omega''} = 2.2$ kcal mol $^{-1}$ obtained by calculation of conformational energies, which reproduces also the experimental results of unperturbed dimensions measured for this polymer 16 (i.e., $C_n \approx 10$ for heterotactic samples with $w_m \approx 0.4-0.5$).

According to the present data, the chain of PS in the PS-PMMA copolymer seems to suffer a substantial conformational change when it is dissolved in dioxane, indicated by a strong decrease of its anisotropy that becomes roughly half that in CCl $_4$. As Figure 4 shows, this value of $\langle \gamma^2 \rangle/x$ can only be reproduced with positive values of the conformational energy E_η in the range 0.4–0.5 kcal mol $^{-1}$. On the other hand, when the PS chain links two segments of PMMA as in the PMMA-PS-PMMA block copolymer, it also undergoes a change in the conformational equilibrium, although this time in the opposite sense, with $\langle \gamma^2 \rangle/x$ increasing by almost a factor of 2. Again Figure 4 indicates that this anisotropy can be reproduced with more negative values of E_η in the range -0.6 to -1.5 kcal mol $^{-1}$.

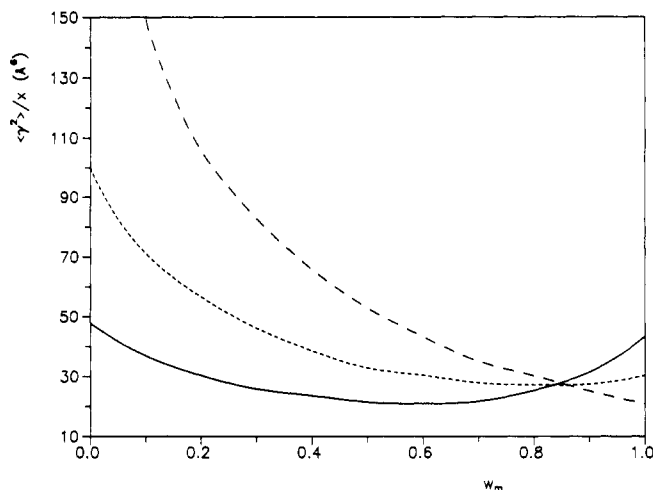


Figure 6. Mean-square optical anisotropy per repeat unit $\langle \gamma^2 \rangle/x$ as a function of the fraction of meso diads w_m . Computations were performed at 25 °C with $E_\omega = E_{\omega'} = 2.0$ kcal mol $^{-1}$ and $E_\eta = 0.4$, $E_{\omega''} = 2.0$ kcal mol $^{-1}$ (solid line); $E_\eta = -0.4$, $E_{\omega''} = 2.2$ kcal mol $^{-1}$ (dotted line); and $E_\eta = -0.8$, $E_{\omega''} = 1.0$ kcal mol $^{-1}$ (dashed line). Results shown for $0 < w_m < 1.0$ are averages over 20 independently generated Monte Carlo chains with standard errors on the average of ca. 1–2%.

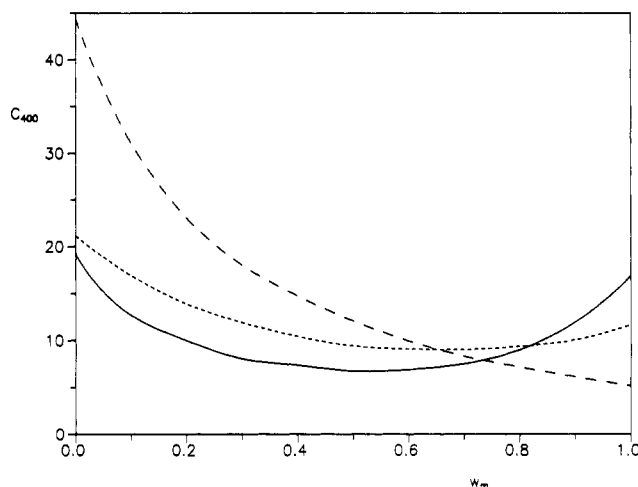


Figure 7. Characteristic ratios $\langle r^2 \rangle_0/nl^2$ for chains containing $n = 400$ skeletal bonds (i.e., $x = n/2 = 200$ repeat units) as a function of the fraction of meso diads. See legend for Figure 6.

Figures 6 and 7 show, respectively, the variation of $\langle \gamma^2 \rangle/x$ and C_n with the tacticity, represented by the fraction of meso diads w_m , for three sets of conformational energies E_η and $E_{\omega''}$ chosen to reproduce the three experimental values of anisotropy obtained for this polymer in different experimental situations. Thus, solid lines in these figures represent values computed with $E_\eta = 0.4$ and $E_{\omega''} = 2.0$ kcal mol $^{-1}$ (set III) that produces $\langle \gamma^2 \rangle/x \approx 24-21$ Å 3 and $C_n \approx 7.4-6.8$ for heterotactic chains with w_m in the range 0.4–0.5. The dotted lines were obtained with the standard set of values $E_\eta = -0.4$ and $E_{\omega''} = 2.2$ kcal mol $^{-1}$ (set II) that was previously used by Flory and co-workers 6,16 giving $\langle \gamma^2 \rangle/x \approx 39-33$ Å 3 and $C_n \approx 10.4-9.6$ with w_m in the range 0.4–0.5. Finally, the dashed lines show the results calculated with $E_\eta = -0.8$ and $E_{\omega''} = 2.0$ kcal mol $^{-1}$ (set I) for which $\langle \gamma^2 \rangle/x \approx 66-53$ Å 3 and $C_n \approx 14.7-12.0$ in the same range of tacticities. Again a comparison between Figures 6 and 7 shows a very direct correlation between the molecular dimension of the chain and its anisotropy.

The kind of conformational changes produced in the polymeric chain from one set of conformational energies to another can be easily understood with the results

Table II
Statistical Weights Computed at 25 °C with $E_{\omega} = E_{\omega'} = 2.0$ kcal mol⁻¹

state	U_{ij}			$U_{ij}/\sum U_{ij}$		
	set I ^a	set II ^b	set III ^c	set I	set II	set III
m tt	0.333	0.044	0.062	0.338	0.033	0.012
m tg	0.324	0.636	2.456	0.329	0.477	0.467
m gt	0.324	0.636	2.456	0.329	0.477	0.467
m gg	0.005	0.018	0.286	0.005	0.013	0.054
r tt	1.000	1.000	1.000	0.883	0.684	0.138
r tg	0.014	0.028	0.109	0.012	0.019	0.015
r gt	0.014	0.028	0.109	0.012	0.019	0.015
r gg	0.105	0.405	6.030	0.093	0.277	0.832

^a Set I: $E_{\eta} = -0.8$; $E_{\omega''} = 1.0$ kcal mol⁻¹. ^b Set II: $E_{\eta} = -0.4$; $E_{\omega''} = 2.2$ kcal mol⁻¹. ^c Set III: $E_{\eta} = 0.4$; $E_{\omega''} = 2.0$ kcal mol⁻¹.

gathered in Table II whose columns 2–4 show the elements of the U'' matrices for the three sets of energies. Columns 5–7 in this table contain the same elements but after renormalization as to give $\sum U_{ij} = 1$. Focusing first on the meso diad, Table II shows that in the case of set III, tg and gt are the preferred states so that an isotactic chain will be formed mainly by helical segments in tg or gt conformations interrupted by gg and, occasionally, by tt units; however, each time that a gg conformation appears, the propagation of the chain suffers an abrupt change of direction; consequently, both the size and the anisotropy of the whole polymer are relatively small. When moving to set II and set I, the preference for tg and gt decreases slightly while the weight of tt increases and that of gg becomes almost negligible; thus, both C_n and $\langle \gamma^2 \rangle/x$ rise when the energies change from set III to set I. The changes are more drastic in the case of the racemic diad, where the statistical weights of tg and gt conformations are roughly the same for the three sets of energies, so that moving from set III to set I means a change from a strong preference for gg in set III to an even stronger predilection for tt in set I. Thus, a syndiotactic polymer will have preference for gg conformations, but this sequence cannot perpetuate across the CH₂–C–CH₂ pair of bonds ($U'_{gg} = 0$) and therefore the chain will be essentially an alternation of gg and tt conformations. Moving to sets II and I means the elimination of compact gg units in favor of the most extended and anisotropic tt conformations and, conse-

quently, the dimensions and anisotropy of the chain rise sharply.

We therefore conclude that the differences in the anisotropy exhibited by the PS chain indicate a conformational change produced mainly in the racemic units that changes from a strong preference for gg in the case of PS–PMMA diblock copolymer to a predilection for tt in the PMMA–PS–PMMA copolymer.

Acknowledgment. We thank Dr. P. Lutz for providing us with the block copolymers.

References and Notes

- (1) Fytas, G.; Floudas, G.; Hadjichristidis, N. *Polym. Commun.* **1988**, *29*, 322.
- (2) Floudas, G.; Fytas, G.; Momper, B.; Saiz, E. *Macromolecules* **1990**, *23*, 498.
- (3) Floudas, G.; Lappas, A.; Fytas, G.; Meier, G. *Macromolecules* **1990**, *23*, 1747.
- (4) Floudas, G.; Patkowski, A.; Fytas, G.; Ballauff, M. *J. Phys. Chem.* **1990**, *94*, 3215.
- (5) Flory, P. J. *Statistical Mechanics of Chain Molecules*; Interscience: New York, 1969.
- (6) Suter, U. W.; Flory, P. J. *J. Chem. Soc., Faraday Trans. 2* **1977**, *73*, 1521.
- (7) Tsunashima, Y. *Macromolecules* **1990**, *23*, 2963 and references therein.
- (8) Tanaka, T.; Kotaka, T.; Inagaki, H. *Macromolecules* **1976**, *9*, 561.
- (9) Han, C. C.; Mozer, B. *Macromolecules* **1977**, *10*, 44.
- (10) Tanaka, T.; Kotaka, T.; Ban, K.; Hattori, M.; Inagaki, H. *Macromolecules* **1977**, *10*, 960.
- (11) In a paper by Ehrenburg et al. (Ehrenburg, E. G.; Piskareva, E. P.; Poddubnyi, I. Ya. *J. Polym. Sci., Polym. Symp.* **1973**, *42*, 1021), it was claimed that the total depolarized scattering intensity can be utilized to probe defects in a polystyrene–polybutadiene copolymer chain.
- (12) See refs 2 and 4 for a discussion of the ill-conditioned local field problems and the effect of the collision-induced depolarized scattering.
- (13) Floudas, G.; Fytas, G. In *Reactive and Flexible Molecules in Liquids*; Dorfmueller, Th., Ed.; Kluwer Academic: Dordrecht, 1989; p 239.
- (14) Saiz, E.; Suter, U. W.; Flory, P. J. *J. Chem. Soc., Faraday Trans. 2* **1977**, *73*, 1538.
- (15) Huber, K.; Bantle, S.; Lutz, P.; Burchard, W. *Macromolecules* **1985**, *18*, 1461 and references therein.
- (16) Yoon, D. Y.; Sundararajan, P. R.; Flory, P. J. *Macromolecules* **1975**, *6*, 776.
- (17) Flory, P. J. *Macromolecules* **1974**, *7*, 381.

Registry No. (PMMA)(PS) (block copolymer), 106911-77-7.